Organic LETTERS

Letter

pubs.acs.org/OrgLett

Conformationally Locked Tolans, β-Sheet Structures, and Photophysical Properties

Jung-Ho Hong,[†] Ananta Kumar Atta,[†,§] Kwang-Bok Jung,[†] Seul-Bi Kim,[†] Jungseok Heo,[‡] and Dong-Gyu Cho*[,†]

[†]Department of Chemistry, Inha University, 253 Yonghyundong, Namgu, Incheon 402-751, Republic of Korea

[‡]Department of Chemistry, Chungnam National University, 99 Daehak-ro, Yuseong-go, Daejeon 305-764, Republic of Korea

Supporting Information

ABSTRACT: Conformationally locked tetrasubstituted tolans were synthesized by introducing a tether on the tolan. To demonstrate the utilities of these motifs, a β-hairpin structure (**15**) was synthesized, and its additional stabilizing effects were evaluated. Moreover, the photophysical properties of cyclic tolans and their β-sheet structure were investigated. The fluorescence quantum yield of cyclic tolan **12** is >1000 times stronger than its congener **1** in CH_3CN.

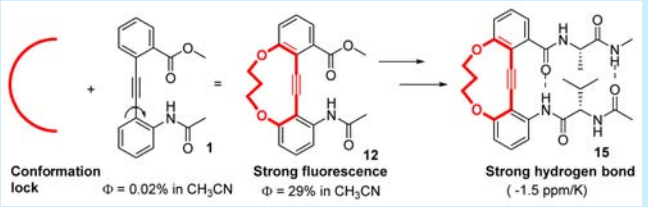

Diphenylacetylene, commonly known as tolan, has an infinite number of conformers around its acetylene axis. This property can be modulated by either weak interactions such as hydrogen bonds or strong interactions such as covalent bonds. The structures and their properties have been widely studied as scaffolds for rotors,[1] switches,[2] sensors,[3] foldamers,[4] and β-turn mimics.[5] They also have interesting photophysical properties.[6] Among them, β-turn mimics based on tolans require a conformational lock using hydrogen bonds between the two strands attached to the tolan. These strategies were first utilized by Kemp.[5] The propensity of tolans to form a β-sheet structure was qualitatively investigated using dipeptides, as shown in Scheme 1. The same compound, including its diastereoisomer,

Scheme 1. Schematic Representation of Conformationally Locked and Unlocked Aryl-Based β-Turns

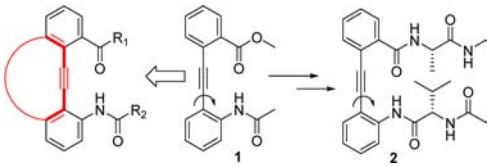

was resynthesized by Gogoll.[7] The β-sheet structures of the two diastereoisomers were quantitatively reinvestigated. Later, Kemp's motifs were incorporated into cyclic peptides by Spivey to mimic the human immunoglobulin E.[8] However, the unique properties of cyclic tolans have not been fully utilized. Tolan can be modified to conformationally and geometrically well-defined synthetic motifs possessing unique fluorescence properties, even though some of the cyclic tolans are known and have a certain degree of fluorescence properties.[9] Herein, for the first time, cyclic tolans were synthesized as structurally preorganized motifs; the functionalizable cyclic tolans were further modified to a β-sheet structure. Moreover, their photophysical properties were evaluated.

To prevent the formation of undesired conformations of tolans and evaluate the effects of substituents on their fluorescence properties, an 11-membered macrocyclic tetrasubstituted tolan was designed to act as a motif for β-turn mimics. The diphenylacetylene core has been synthesized previously using Sonogashira coupling,[5] alkyne metathesis,[9] and elimination of dibromoalkanes.[10] In this study, Sonogashira coupling was used, even though the Sonogashira coupling of highly functionalized 2,6-disubstituted iodobenzene and 2,6-disubstituted ethynylbenzene has been rarely reported. As shown in Scheme 2, the first step in the synthesis of the macrocycle was the iodination of methyl 2-amino-3-hydroxybenzoate **3**.[11] The iodinated compound **4** underwent Sonogashira coupling with TMS-acetylene, affording compound **5** in 83% yield. The acetylation of compound **5** followed by fluoride-ion-induced desilylation afforded compound **6** in 92% yield. Next, compound **6** was coupled with 2-iodo-3-nitrophenol, affording the main diphenylacetylene skeleton **7** in a moderate yield. Product **7** was converted to bromide **8** via a Williamson ether synthesis. Subsequent deacetylation of bromide **8** followed by the cyclization of **9** afforded macrocycle **10** in an excellent yield. The nitro group of macrocycle **10** was reduced to the amine group, affording compound **11** in 83% yield. Finally, amide derivative **12** was obtained from compound **11** under typical acylation conditions.

All of the compounds were characterized using ^{1}H NMR, ^{13}C NMR, 2D NOESY spectra, and high-resolution mass analysis. Fortunately, a single crystal of compound **12**[12] was obtained by the slow evaporation of a mixture of ethyl acetate and *n*-hexane. The X-ray diffraction analysis of compound **12** showed that the

Received: November 6, 2015
Published: December 3, 2015

DOI: 10.1021/acs.orglett.5b03205
Org. Lett. 2015, 17, 6222−6225

Scheme 2. Synthesis of Cyclic Tolans 11 and 12

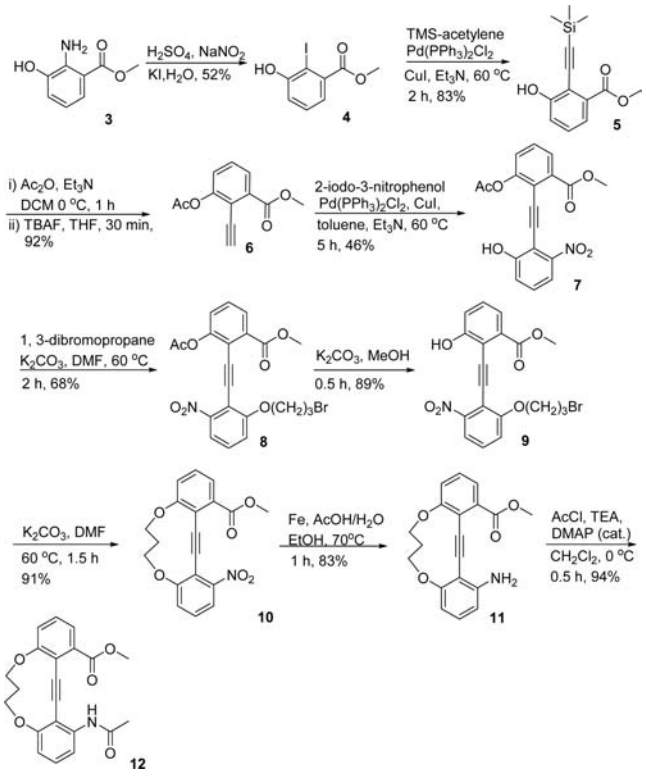

ether tether efficiently restricted the free rotation of the two phenyl groups. Moreover, macrocycle **12** also showed hydrogen bonding in the solid state, with relatively longer H-bond lengths (N···H···O = 3.33 Å). The induced coplanarity of the two phenyl groups was deduced from the dihedral angle of ca. 16° between the two phenyl groups, even though the overall molecule is almost flat (*i.e.*, in the same plane) from the top view, as shown in Figure 1.

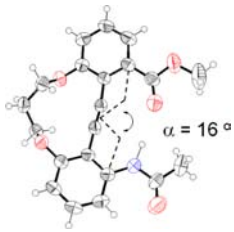

Figure 1. X-ray crystal structures of the side views of macrocycle **12**, showing the dihedral angle between the phenyl groups. Thermal ellipsoids are scaled to the 50% probability level.

To evaluate the effects of the cyclic tolan in stabilizing the β-sheet structure and directly compare β-sheet **2**, amino acid **13** was used in standard amide-bond-forming reactions with alanine and valine derivatives to produce peptide **15**, as shown in Scheme 3. β-Hairpin **15** was enantioselectively synthesized from macrocycle **11**. However, a simple hydrolysis of the ester group on tolan caused racemization of the introduced amino acid residues.[7] To avoid the racemization of the first strand, Spivey et al. first reduced the ester group of tolan to an alcohol and then oxidized the alcohol to form an acid.[8b] However, the above protocol was not easily applicable, especially in the last stage of our synthesis. After repeated failures, we observed that the

Scheme 3. Synthesis of Short β-Hairpin 15 and 16

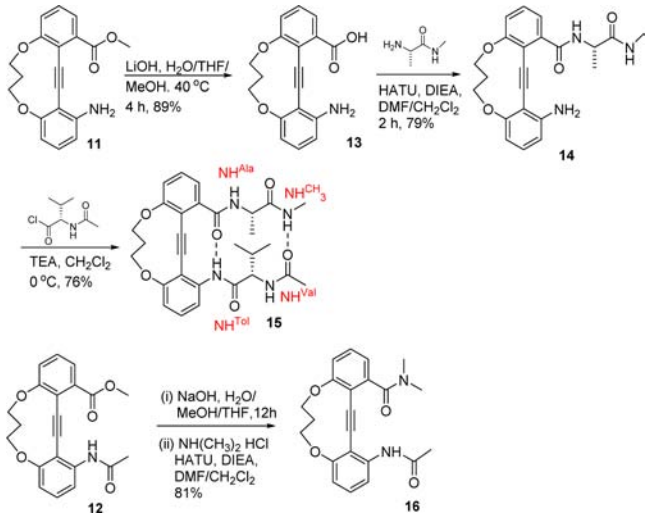

aromatic amine group in macrocycle **11** was not reactive in a typical amide-forming reaction. Instead, ester **11** was subjected to hydrolysis followed by two consecutive typical amide-bond-forming reactions in the absence of any protection group, thus successfully affording the enantiomerically pure short β-turn mimetic **15** via compounds **13** and **14**, as shown in Scheme 3. To compare the effects of substituents on the tolan, compound **16** was separately synthesized.

To evaluate the stabilizing effect of **11**, the temperature coefficients of the amide NH protons of compounds **1**, **2**, **12**, and **15** were compared in DMSO-d_6 (Table 1). When the

Table 1. Temperature Coefficients (ppb/K) of the Amide NH Protons in Compounds 1, 2, 12, and 15

	NH^{tol}	NH^{ala}	NH^{val}	NH^{CH_3}
1	−2.7			
2[a]	−3.1	−5.9	−5.3	−4.5
12	−2.4			
15	−1.5	−6.0	−5.6	−4.7

[a]Values were obtained from the literature.[7]

unfunctionalized tolan motif **1** was incorporated into the short β-turn mimic **2**, the temperature coefficient of the NH^{tol} proton decreased from −2.7 ppb/K for compound **1** to −3.1 ppb/K for compound **2** according to the literature reports[7] and our results (Figures S4 and S5 in the Supporting Information). In contrast, the temperature coefficient of the NH^{tol} proton increased from −2.4 ppb/K for compound **12** to −1.5 ppb/K for compound **15** (Figures S8 and S9). Such high values for the temperature coefficient of the NH^{tol} proton in compound **15** are unprecedented in noncyclic β-sheet structures. Such large values were often observed in small cyclic pentapeptides (β, γ, or γ, γ turns).[13,14] The large temperature coefficient of the NH^{tol} proton in compound **15** can be attributed to the increased hydrogen bonding between CO^{tol} and NH^{tol} because the cyclic 11-membered motif forced the two strands to come closer.[15] In addition, the effect of cyclic tolan was also observed at the ends of the two strands of **15**. For example, the chemical shift of NH^{CH_3} in compounds **15**, **14**, and **2**[7] were 7.96, 7.91, and 7.91 ppm, respectively (Figure S10). The chemical shift of NH^{CH_3} of **15** shifted downfield by δ 0.05 ppm compared to compounds **2** and **14** in DMSO-d_6. Moreover, the NH^{CH_3} chemical shift in

DOI: 10.1021/acs.orglett.5b03205
Org. Lett. 2015, 17, 6222−6225

compound **14** is exactly the same as that observed in compound **2**, despite the fact that the NH^{CH_3} proton of **14** did not participate in any intramolecular hydrogen bonding. The NH^{CH_3} protons in compounds **14** and **2** are very far from the tolan motif; therefore, the observed chemical shifts should depend directly on the strength of the hydrogen bond of the NH^{CH_3} protons in the same solvent. Thus, the terminal groups on the chain in compound **15** exhibited hydrogen bonding at 25 °C relatively stronger than that in compounds **2** and **14**, even though the NH^{CH_3} proton in compound **15** is more solvent-accessible than the NH^{tol} proton. Because the NH^{ala} and NH^{val} protons did not participate in hydrogen bonding, these results partly confirm the stabilizing effect of the cyclic tolan on the formations of β-sheets. Moreover, the hydrogen bonding between the NH^{tol} and CO of compounds **2** and **15** played a pivotal role in maintaining hairpin-like structures.

The secondary structure of compound **15** can be inferred from the 2D NOESY spectra in DMSO-d_6 and $CDCl_3$ (Figures S2 and S3). The presence of two antiparallel strands in DMSO-d_6 is evident from the appearance of three pairs of correlation peaks (NH^{ala}–CH^{tol}, α-CH^{ala}–NH^{CH_3}, and α-CH^{val}–NH^{tol}) in the spectrum. The α-CH^{val}–$CH_3{}^{ala}$ and α-CH^{val}–α-CH^{ala} correlation peaks were only observed in the antiparallel β-sheets. Although similar cross-peaks were observed in $CDCl_3$, further detailed analysis was not possible because of the two overlapped chemical shifts of α-CH^{val} and α-CH^{ala} protons. Unfortunately, a good-quality crystal of compound **15** could not be obtained.

The photophysical properties of the cyclic β-turn mimic motif and sheet were characterized from the normalized absorbance and fluorescence spectra. Figure 2a shows the absorption maxima

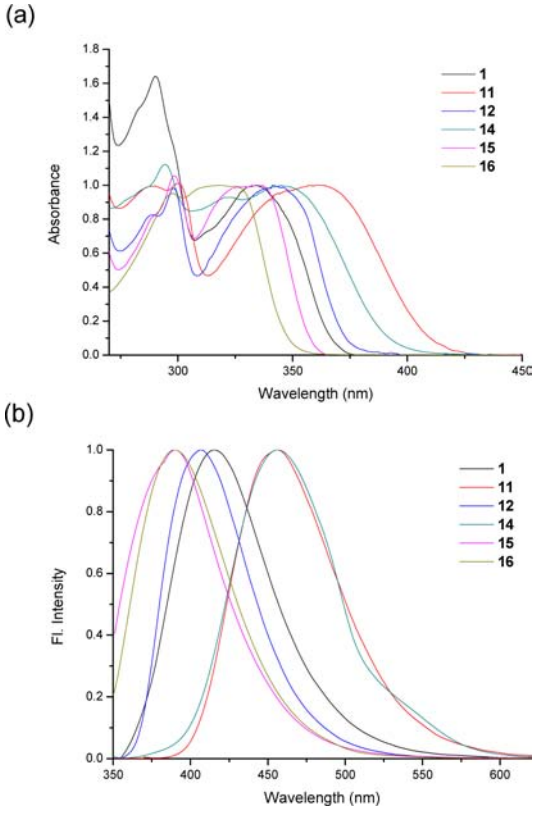

Figure 2. (a) Normalized UV–visible absorption spectra of compounds **1**, **11**, **12**, **14**, **15**, and **16** in CH_2Cl_2. (b) Normalized emission spectra of compounds **1**, **11**, **12**, **14**, **15**, and **16** in CH_2Cl_2.

($^{abs}\lambda_{max}$) of the compounds. The $^{abs}\lambda_{max}$ values of compounds **12** and **15** were blue-shifted by 47 and 63 nm, respectively, when the amine group in compound **11** was functionalized with acetyl chloride and two amino acids. Such bathochromic shifts are commonly observed for intramolecular charge-transfer (ICT) molecules. The solutions of macrocycles **11** and **12** showed strong fluorescence under a laboratory hand-held UV lamp at 365 nm, as inferred from the fluorescent spectra shown in Figures 2b and S11. The fluorescence quantum yield of each compound was determined relative to that of Coumarin-120 in CH_2Cl_2[16] and CH_3CN.[17] The values obtained are also summarized in Table 2. The quantum yields of the molecules in CH_2Cl_2

Table 2. Spectroscopic Data and Quantum Yields of 1, 11, 12, 14, 15, and 16 in CH_2Cl_2

	1	11	12	14	15	16
$^{abs}\lambda_{max}$	334	363	341	345	336	318
ε	16100	12700	14300	10386	19700	21667
$^{em}\lambda_{max}$	419	453	406	456	390	390
Stokes shift	85	90	65	107	54	72
Φ (%)	0.03	14	33	44	3	1.2
Φ (%)[a]	0.02	3	29	25	2	0.5

[a]Quantum yield was obtained in CH_3CN. Unspecified units are nm except ε (cm^{-1} M^{-1}).

decreased in the order **14** > **12** > **11** > **15** > **16**. The quantum yield trends are difficult to rationalize. However, the first functional groups of the two strands are pivotal for the fluorescence quantum yields of the compounds. Typically, when the first two functional groups are amide groups, the quantum yields significantly decreased. Both the quantum yields of compounds **11** and **14** decreased in the more polar solvent CH_3CN. This trend can be attributed to favorable interactions between strong ICT compounds and polar solvents in the excited states.[18] Because a larger Stokes shift was observed for compounds **11** and **14** (Table 2), probably macrocycles **11** and **14** possess a larger charge-transfer character.[19] Thus, the quantum yield of compound **11** was large in CH_2Cl_2 but decreased in CH_3CN. In general, the large quantum yields observed for these molecules may result from the restricted free rotation and induced planarity[6] and from the effects of substituents on the cyclic tolan. In contrast, the excited state of compound **1** did not show fluorescence properties via the nonradiative loss of rotational energy.

In conclusion, unlike a simple tolan (free rotation around its acetylene axis), cyclic tolans were synthesized by introducing a tether to connect the two phenyl groups on the tolan. In this manner, the cyclic tolans were obtained as structurally preorganized motifs, and the functionalizable cyclic tolans were further modified to a β-sheet structure. The stability of the β-sheet structure was determined from the temperature coefficients of the amide protons. The hydrogen bond between the amide and carbonyl groups closest to the cyclic β-turn motif was as strong as the hydrogen bonds often found in small cyclic pentapeptides (β, γ, or γ, γ turns). In addition, the corresponding cyclic derivative **12** exhibited fluorescence 1000-fold stronger than its precursor **1** (a simple tolan). It should be emphasized again that cyclic tolans have a completely opposite potential of the tolans so far used in many applications. The above studies indicate that cyclic tolans can be used as conformationally and geometrically well-defined motifs such as hexasubstituted benzene,[20] Kemp's triacid,[21] and Troger's base.[22] Unlike these

DOI: 10.1021/acs.orglett.5b03205
Org. Lett. 2015, 17, 6222–6225

known motifs, cyclic tolans possess inherent fluorescence. More research on functionalized cyclic tolans is underway.

■ ASSOCIATED CONTENT

Supporting Information

The Supporting Information is available free of charge on the ACS Publications website at DOI: 10.1021/acs.orglett.5b03205.

Experimental procedures, characterization data, and ^{1}H and ^{13}C NMR spectra for all compounds (PDF)
X-ray data of **12** (CIF)

■ AUTHOR INFORMATION

Corresponding Author

*E-mail: dgcho@inha.ac.kr.

Present Address

[§](A.K.A.) National Institute of Technology Arunachal Pradesh, Yupia, India 791112.

Notes

The authors declare no competing financial interest.

■ ACKNOWLEDGMENTS

This research was supported by the Basic Science Research Program through the National Research Foundation of Korea (NRF), funded by the Ministry of Education, Science and Technology (Grant No. NRF-2013R1A1A2057508). We would like to thank Dr. Kun Cho from the mass spectrometry lab of the Korea Basic Science Institute for MS analysis.

■ REFERENCES

(1) (a) Karim, A. R.; Linden, A.; Baldridge, K. K.; Siegel, J. S. *Chem. Sci.* **2010**, *1*, 102. (b) Godinez, C. E.; Zepeda, G.; Garcia-Garibay, M. A. *J. Am. Chem. Soc.* **2002**, *124*, 4701.

(2) (a) Jones, I. M.; Hamilton, A. D. *Org. Lett.* **2010**, *12*, 3651. (b) Jones, I. M.; Hamilton, A. D. *Angew. Chem., Int. Ed.* **2011**, *50*, 4597.

(3) (a) Jo, J.; Lee, D. *J. Am. Chem. Soc.* **2009**, *131*, 16283. (b) Atta, A. K.; Ahn, I.-H.; Hong, A.-Y.; Heo, J.; Kim, C. K.; Cho, D.-G. *Tetrahedron Lett.* **2012**, *53*, 575.

(4) Cary, J. M.; Moore, J. S. *Org. Lett.* **2002**, *4*, 4663.

(5) (a) Kemp, D. S.; Li, Z. Q. *Tetrahedron Lett.* **1995**, *36*, 4175. (b) Kemp, D. S.; Li, Z. Q. *Tetrahedron Lett.* **1995**, *36*, 4179.

(6) (a) Swinburne, A. N.; Paterson, M. J.; Beeby, A.; Steed, J. W. *Chem. - Eur. J.* **2010**, *16*, 2714. (b) Menning, S.; Krämer, M.; Coombs, B. A.; Rominger, F.; Beeby, A.; Dreuw, A.; Bunz, U. H. F. *J. Am. Chem. Soc.* **2013**, *135*, 2160.

(7) Erdélyi, M.; Langer, V.; Karlén, A.; Gogoll, A. *New J. Chem.* **2002**, *26*, 834.

(8) (a) Spivey, A. C.; McKendrick, J.; Srikaran, R.; Helm, B. A. *J. Org. Chem.* **2003**, *68*, 1843. (b) Offermann, D. A.; McKendrick, J. E.; Sejberg, J. J. P.; Mo, B.; Holdom, M. D.; Helm, B. A.; Leatherbarrow, R. J.; Beavil, A. J.; Sutton, B. J.; Spivey, A. C. *J. Org. Chem.* **2012**, *77*, 3197.

(9) Brizius, G.; Billingsley, K.; Smith, M. D.; Bunz, U. H. F. *Org. Lett.* **2003**, *5*, 3951.

(10) Darabi, H. R.; Jadidi, K.; Mohebbi, A. R.; Faraji, L.; Aghapoor, K.; Shahbazian, S.; Azimzadeh, M.; Nasseri, S. M. *Supramol. Chem.* **2008**, *20*, 327.

(11) Fielder, D. A.; Collins, F. W. *J. Nat. Prod.* **1995**, *58*, 456.

(12) CCDC 902556 and 902557 (**11** and **12**, respectively) contain the supplementary crystallographic data for this paper. The obtained crystal data of **11** were not good enough to discuss here. These data can be obtained free of charge from the Cambridge Crystallographic Data Centre via www.ccdc.cam.ac.uk/data_request/cif.

(13) Kessler, H. *Angew. Chem., Int. Ed. Engl.* **1982**, *21*, 512.

(14) (a) Pease, L. G.; Watson, C. *J. Am. Chem. Soc.* **1978**, *100*, 1279. (b) Weißhoff, H.; Präsang, C.; Henklein, P.; Frömmel, C.; Zschunke, A.; Mügge, C. *Eur. J. Biochem.* **1999**, *259*, 776.

(15) Amide NH bonds of **1** and **12** were also examined by infrared spectroscopy. The intensity of both NH (hydrogen-bonded) bonds are almost identical, while both of the non-hydrogen-bonded NHs are not clearly seen in the spectra. Therefore, the strength of the hydrogen bonds of **1** and **12** cannot be compared by IR spectra (Figure S19). See: Díaz, H.; Espina, J. R.; Kelly, J. W. *J. Am. Chem. Soc.* **1992**, *114*, 8316.

(16) Park, S.-Y.; Ebihara, M.; Kubota, Y.; Funabiki, K.; Matsui, M. *Dyes Pigm.* **2009**, *82*, 258.

(17) Pal, H.; Nad, S.; Kumbhakar, M. *J. Chem. Phys.* **2003**, *119*, 443.

(18) Shao, J.; Guan, Z.; Yan, Y.; Jiao, C.; Xu, Q.-H.; Chi, C. *J. Org. Chem.* **2011**, *76*, 780.

(19) Bhaskar, A.; Ramakrishna, G.; Lu, Z.; Twieg, R.; Hales, J. M.; Hagan, D. J.; Van Stryland, E.; Goodson, T. *J. Am. Chem. Soc.* **2006**, *128*, 11840.

(20) (a) Stack, T. D. P.; Hou, Z.; Raymond, K. N. *J. Am. Chem. Soc.* **1993**, *115*, 6466. (b) Rekharsky, M.; Inoue, Y.; Tobey, S.; Metzger, A.; Anslyn, E. *J. Am. Chem. Soc.* **2002**, *124*, 14959. (c) Ustinov, A.; Weissman, H.; Shirman, E.; Pinkas, I.; Zuo, X.; Rybtchinski, B. *J. Am. Chem. Soc.* **2011**, *133*, 16201.

(21) (a) Rebek, J.; Askew, B.; Killoran, M.; Nemeth, D.; Lin, F. T. *J. Am. Chem. Soc.* **1987**, *109*, 2426. (b) Zhang, X.-X.; Lippard, S. J. *J. Org. Chem.* **2000**, *65*, 5298. (c) Shenoy, S. R.; Pinacho Crisóstomo, F. R.; Iwasawa, T.; Rebek, J. *J. Am. Chem. Soc.* **2008**, *130*, 5658.

(22) (a) Adrian, J. C., Jr.; Wilcox, C. S. *J. Am. Chem. Soc.* **1989**, *111*, 8055. (b) Boyle, E. M.; Comby, S.; Molloy, J. K.; Gunnlaugsson, T. *J. Org. Chem.* **2013**, *78*, 8312.

DOI: 10.1021/acs.orglett.5b03205
Org. Lett. 2015, 17, 6222−6225